The BiPo-3 detector

A.S. Barabash[a], A. Basharina-Freshville[b,c], S. Blondel[d], S. Blot[c], M. Bongrand[d], D. Boursette[d], V. Brudanin[e], J. Busto[f], A.J. Caffrey[g], S. Calvez[d], M. Cascella[b], C. Cerna[h], E. Chauveau[h], A. Chopra[b], S. De Capua[c], D. Duchesneau[i], V. Egorov[e], G. Eurin[d,b], J.J. Evans[c], L. Fajt[j], D. Filosofov[e], R. Flack[b], X. Garrido[d], H. Gómez[d], B. Guillon[k], P. Guzowski[c], K. Holý[l], R. Hodák[b], A. Huber[h], C. Hugon[h], A. Jeremie[i], S. Jullian[d], M. Kauer[b], A. Klimenko[e], O. Kochetov[e], S.I. Konovalov[a], V. Kovalenko[e], K. Lang[m], Y. Lemière[k], T. Le Noblet[i], Z. Liptak[m], X.R. Liu[b], P. Loaiza,[d,*], G. Lutter[h], M. Macko[l], F. Mamedov[j], C. Marquet[h], F. Mauger[k], B. Morgan[n], J. Mott[b], I. Nemchenok[e], M. Nomachi[o], F. Nova[m], H. Ohsumi[p], R.B. Pahlka[m], J. Pater[c], F. Perrot[h], F. Piquemal[h,q], P. Povinec[l], P. Přidal[j], Y.A. Ramachers[n], A. Remoto[i], B. Richards[b], C.L. Riddle[g], E. Rukhadze[j], R. Saakyan[b], X. Sarazin[d], Yu. Shitov[e,r], L. Simard[d,s], F. Šimkovic[l], A. Smetana[j], K. Smolek[j], A. Smolnikov[e], S. Söldner-Rembold[c], B. Soulé[h], I. Štekl[j], J. Thomas[b], V. Timkin[e], S. Torre[b], Vl.I. Tretyak[t], V.I. Tretyak[e], V.I. Umatov[a], C. Vilela[b], V. Vorobel[u], D. Waters[b], A. Žukauskas[u]

[a] *NRC "Kurchatov Institute", ITEP, 117218 Moscow, Russia*
[b] *University College London, London WC1E 6BT, United Kingdom*
[c] *University of Manchester, Manchester M13 9PL, United Kingdom*
[d] *LAL, Université Paris-Sud, CNRS/IN2P3, Université Paris-Saclay, F-91405 Orsay, France*
[e] *JINR, 141980 Dubna, Russia*
[f] *Aix Marseille Univ., CNRS, CPPM, Marseille, France*
[g] *Idaho National Laboratory, Idaho Falls, ID 83415, United States*
[h] *CENBG, Université de Bordeaux, CNRS/IN2P3, F-33175 Gradignan, France*
[i] *LAPP, Université de Savoie, CNRS/IN2P3, F-74941 Annecy-le-Vieux, France*
[j] *Institute of Experimental and Applied Physics, Czech Technical University in Prague, CZ-12800 Prague, Czech Republic*
[k] *LPC Caen, ENSICAEN, Université de Caen, CNRS/IN2P3, F-14050 Caen, France*
[l] *FMFI, Comenius University, SK-842 48 Bratislava, Slovakia*
[m] *University of Texas at Austin, Austin, TX 78712, United States*
[n] *University of Warwick, Coventry CV4 7AL, United Kingdom*
[o] *Osaka University, 1-1 Machikaney arna Toyonaka, Osaka 560-0043, Japan*
[p] *Saga University, Saga 840-8502, Japan*
[q] *Laboratoire Souterrain de Modane, F-73500 Modane, France*
[r] *Imperial College London, London SW7 2AZ, United Kingdom*
[s] *Institut Universitaire de France, F-75005 Paris, France*
[t] *Institute for Nuclear Research, MSP 03680 Kyiv, Ukraine*
[u] *Charles University, Prague, Faculty of Mathematics and Physics, CZ-12116 Prague, Czech Republic*

Abstract

The BiPo-3 detector is a low radioactive detector dedicated to measuring ultra-low natural contaminations of ^{208}Tl and ^{214}Bi in thin materials, initially developed to measure the radiopurity of the double β source foils of the SuperNEMO experiment at the μBq/kg level. The BiPo-3 technique consists in installing the foil of interest between two thin ultra-radiopure scintillators coupled to low radiactive photomultipliers. The design and performances of the detector are presented.

In this paper, the final results of the ^{208}Tl and ^{214}Bi activity measurements of the first enriched ^{82}Se foils are reported for the first time, showing the capability of the detector to reach sensitivities in the range of some μBq/kg.

Keywords: low radioactivity measurements, double beta decay detectors

1. Introduction

The BiPo-3 detector, running in the Canfranc Underground Laboratory, Spain, since 2013, has been initially developed to measure ultra low natural contaminations

*Corresponding author

of ^{212}Bi and ^{214}Bi in the SuperNEMO source foils. The goal of the SuperNEMO experiment is to search for the neutrinoless double β decay, $\beta\beta0\nu$ [Arnold et al., 2010] as an experimental proof that the neutrino is a Majorana particle, i.e. identical to its own antiparticle. SuperNEMO will measure 100 kg of $\beta\beta0\nu$ isotopes with a sensitivity of $T_{1/2}(\beta\beta0\nu) > 10^{26}$ years. The baseline isotope is ^{82}Se with a $Q_{\beta\beta}$ value = 2.998 MeV. One of the main sources of background for SuperNEMO is a possible contamination of ^{208}Tl (Q_β = 4.99 MeV) and ^{214}Bi (Q_β = 3.27 MeV) produced inside the $\beta\beta0\nu$ source foils. The required radiopurities of the $\beta\beta0\nu$ foils are $\mathcal{A}(^{208}\text{Tl}) < 2\,\mu$Bq/kg and $\mathcal{A}(^{214}\text{Bi}) < 10\,\mu$Bq/kg in order to achieve the desired SuperNEMO sensitivity [Arnold et al., 2010]. To measure such low levels in the $\beta\beta0\nu$ foils the collaboration has developed the BiPo-3 detector. We show in this paper that the BiPo-3 performances have been achieved: the BiPo-3 detector can measure the radiopurity of double beta metallic foils with a total surface at the level of some μBq/kg. We show also that the BiPo-3 detector becomes a generic low radioactive detector, which can measure the natural radioactivity in Tl and Bi of general thin materials with an unprecedent sensitivity.

2. Measurement principle of the BiPo-3 detector

In order to measure ^{208}Tl and ^{214}Bi contaminations, the underlying concept of the BiPo-3 detector is to detect with organic plastic scintillators the so-called BiPo process, which corresponds to the detection of an electron followed by a delayed α particle [Bongrand et al., 2011], [Gomez et al., 2013]. The ^{214}Bi isotope is a (β,γ) emitter decaying to ^{214}Po, which is an α emitter (E_α=7.69 MeV [Bé et al, 2008]) with a half-life of 162 μs. The ^{208}Tl isotope is measured by detecting its parent, ^{212}Bi. Here ^{212}Bi decays with a branching ratio of 64% [Bé et al, 2004] via a β emission (Q_β = 2.25 MeV) towards the daughter nucleus ^{212}Po which is a pure α emitter (E_α=8.79 MeV [Bé et al, 2004]) with a short half-life of 300 ns, as summarized in Figure 1.

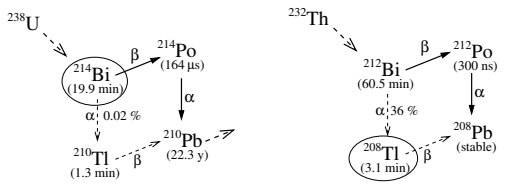

Figure 1: The ^{214}Bi-^{214}Po and ^{212}Bi-^{212}Po cascades used for the ^{214}Bi and ^{208}Tl measurements.

The BiPo-3 experimental technique consists in installing the foil of interest between two thin ultra radiopure organic plastic scintillators, as illustrated in Figure 2. The ^{212}Bi (^{208}Tl) and ^{214}Bi contaminations inside the foil are measured by detecting the β decay followed by the delayed α particle within a time window which depend on the isotope to be measured. The energy of the delayed α particle provides information on whether the contamination is on the surface or in the bulk of the foil.

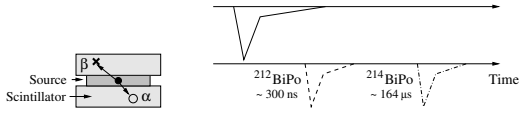

Figure 2: Schematic view of the BiPo detection technique with the source foil inserted between two plastic scintillators plate, and the scintillation signal waveforms acquired for a BiPo event. The prompt β signal and the delayed α signal observed by the top and bottom scintillators respectively are schematically illustrated.

3. Description of the BiPo-3 detector

The detector is composed of two modules. Each module (see Figure 3) consists of 20 pairs of optical submodules, positioned in two rows. Each optical submodule consists of a scintillator plate coupled with a polymethyl methacrylate (PMMA) optical guide to a 5 inches low radioactive photomultipliers [Bongrand et al., 2011]. The optical sub-modules are arranged face-to-face to form a pair . The size of each scintillator is 300×300×2 mm^3. The BiPo-3 detector corresponds to a total number of 80 optical sub-modules and a total detector surface of 3.6 m^2. The surface of the scintillators facing the source foil are covered with a 200 nm thick layer of evaporated ultra radiopure aluminium in order to optically isolate each scintillator from its neighbour, and to improve the light collection efficiency. The two BiPo-3 modules are installed inside a low-radioactivity shield. The shield is built out of a radon-tight stainless steel tank with the upper part composed of a pure iron lid (2 cm thick). Low-activity lead bricks are assembled inside the tank and above the upper iron plate for a total thickness of 10 cm. Pure iron plates, 18 cm thick, are added under the tank and on its lateral sides. The radiopurity of all the materials used for the detector have been measured to ensure high radiopurity. A selection of results is shown in Table 1.

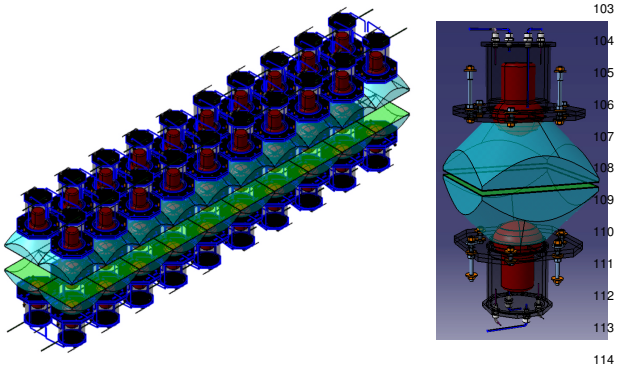

Figure 3: Details of the assembly of the 40 optical sub-modules inside a BiPo-3 module. On the right, a pair of optical sub-modules with the two thin scintillators (in green) face-to-face, coupled with a PMMA optical guide (blue) to a low radioactive 5 inches PMT (red).

Activity (mBq/kg)	^{40}K	^{214}Bi	^{228}Th
Al. on scintillators	-	-	< 0.6
Scintillators	17 ± 2	< 0.1	< 0.1
PMTs	1377	623	104
PMMA	< 109	< 6	< 7
RTV glue 615	491 ± 146	<18	< 11
Iron shield	< 11	< 1	< 3

Table 1: Radioactivity measurements using HPGe of the BiPo-3 components. The mass of one photomultiplier (PMT) is 385 g.

4. Background measurement

4.1. Sources of the background

The first source of background are the random coincidences between two opposite scintillators, giving a background signal within the delay time window, as illustrated in Figure 4 (a). The delay time distribution of the random coincidence is flat and the energy distributions of both the prompt and delayed signals are localized at low energy, since the single counting rate is dominated by Compton electrons due to external γ.

The second source of background comes from ^{212}Bi and ^{214}Bi contaminations on the surface of the scintillator in contact with the sample foil, hereafter called surface background, as illustrated in Figure 4 (b). The delayed α particle, emitted from the surface of the scintillator, deposits all its energy inside the scintillator.

The third potential source of background is the ^{212}Bi or ^{214}Bi bulk contamination inside the scintillator volume. In this case, the delayed α particle deposits also all its energy inside the scintillator but the prompt electron first triggers this scintillator block before escaping and entering the opposite one, as illustrated in Figure 5. Therefore two prompt signals are detected in coincidence in the two opposite scintillators, allowing the rejection of this class of background events.

Thus the background can be defined by two components: the random coincidences and the surface background.

The energy spectrum of the delayed signal is the most sensitive observable to discriminate the two background components. For surface background, the delayed α particle deposits all its energy inside the scintillator, corresponding to a peak at around 800 keV for ^{214}Bi and around 1 MeV for ^{212}Bi, while random coincidence signals are dominant at low energy.

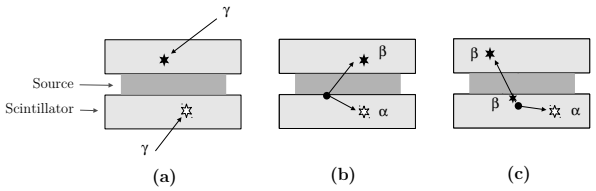

Figure 4: Illustration of the possible sources of background: (a) random coincidences due to the γ flux, (b) ^{212}Bi or ^{214}Bi contamination on the surface of the scintillators, (c) ^{212}Bi or ^{214}Bi contamination in the volume of the scintillators.

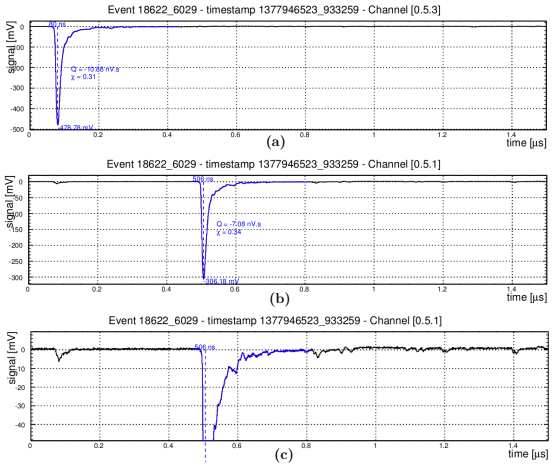

Figure 5: Display of a BiPo event identified as a bulk contamination inside the scintillators, with a signal in coincidence with the prompt signal in the opposite scintillator: (a) the prompt signal, (b) the delayed signal, (c) a zoom of the delayed signal with the coincidence signal. Using the coincidence of the prompt signals, these kind of background events are rejected.

4.2. Measurement conditions

The background is measured by closing the detector, without any sample between the scintillators. Opposite scintillators are directly in contact.

The background has been measured separately for each of the two BiPo-3 modules. The background of the Module 1 has been measured from July 2012 to September 2012 at the begining of the commissioning with a preliminary shield, and from July 2013 to September 2013 with the final shield and after having introduced and measured several samples. The background of Module 2 has been measured from February 2013 to May 2013, with the final shield. The measurements allow to characterize at the same time the backgrounds for ^{212}Bi and ^{214}Bi.

4.3. Event selection

Only the events with β and α particles entering different scintillators on opposite sides of the detection volume, *back-to-back* events, are considered (as the one in Figure 2, left). Events with β and α particles entering in the same scintillator, *same-side* events, are not used since the level of background is much higher than the one measured in the *back-to-back* topology. This is because the bulk contamination inside the scintillators can mimic the *same-side* events.

The coincidence time window for the delay time between the prompt and the delayed signal, Δt, is 20 ns$<\Delta$t$<$1500 ns for ^{212}BiPo events, and 10 μs$<\Delta$t$<$1000 μs for ^{214}BiPo events. The criteria to select the *back-to-back* BiPo events are described in the following. The energy of the prompt signal is greater than 200 keV. The energy of the delayed signal is greater than 150 keV for ^{212}BiPo events, and greater than 300 keV for ^{214}BiPo events. The higher energy threshold for the ^{214}BiPo measurement is set in order to reduce the random coincidence background.. A pulse shape analysis based on the charge over amplitude Q/A ratio of the prompt and delayed signals is applied to reject noise pulses. If a signal greater than 3 mV (about 10 keV) is detected in coincidence with the prompt signal in the opposite scintillator, the BiPo event is recognized as a bulk contamination background event and is rejected (see Figure 5).

4.4. Analysis Method

The observed data is compared to the expected background by fitting simultaneously the energy spectra of the delayed α signal of the two background components. The α energy spectrum of a contamination sitting on the surface of the scintillators is calculated by simulating BiPo decay cascades, uniformely distributed on the surface. The BiPo-3 Monte Carlo simulations are performed with a GEANT4 [Agostinelli et al., 2003] based package using the DECAY0 event generator [Ponkratenko O., Tretyak V. I., Zdesenko Y. ,2000] and the SuperNemo simulation sofware. Detection efficiencies are also obtained from the Monte-Carlo simulations. The detector efficiency for the contamination on the surface of the scintillators, without any sample between, is 32% for ^{212}BiPo events and 28% for ^{214}BiPo events.

The α energy spectrum of the random coincidence background is measured using the single counting events. The rate of random coincidences is also determined independently by measuring the single counting rate of the scintillator plates, using the single counting events. The single rate is calculated by using all the data available and by averaging over all the scintillators. The expected number of random coincidences is equal to $2 \times r_p \times r_d \times \Delta T \times T_{obs}$, where r_p is the single rate measured by applying the prompt energy threshold (200 keV), r_d is the single rate measured by applying the delayed energy threshold (150 keV for ^{212}Bi and 300 keV for ^{214}Bi), ΔT is the time window (1480 ns for ^{212}Bi and 990 μs for ^{214}Bi), and T_{obs} is the duration of the measurement. Comparing the expected number of random coincidences with its fitted value gives a cross-check and a validation of the fitting procedure.

4.5. Result of the background measurements in the ^{212}BiPo and ^{214}BiPo channels

The results of the background measurements in the ^{212}BiPo and ^{214}BiPo channel are presented in Table 2. For ^{212}BiPo, the level of random coincidences, calculated by measuring the single rate, is about 6×10^{-4} counts/day/m^2 of surface area of scintillator, and is negligible. For the ^{214}BiPo measurement, the random coincidence background becomes larger due to the longer ^{214}Po decay half-life, leading to BiPo events with preferentially low energy signals. Therefore an energy threshold of 300 keV on the delayed signal is systematically applied for the ^{214}BiPo measurement. The counterpart is that the ^{214}BiPo efficiency is reduced when measuring samples. The expected rate of random coincidences, calculated by measuring the single rate, as explained in section 4.4, is 0.13 counts/day/m^2 of surface area of scintillator for the first BiPo-3 module with the final shielding, and 0.10 counts/day/m^2 for the second BiPo-3 module. As presented in Table 2, the number of random coincidences estimated by the fit is in agreement with the expected rate calculated from the single rates. It demonstrates the reliability of the fit and the reliability of the estimated activity in ^{214}Bi on the surface of the scintillators.

We note that the levels of surface background measured separately in the two BiPo-3 modules are equal, within the statistical uncertainties (with the exception

of the ^{214}BiPo background measurement with the temporary shielding with a higher surface background, due to a poor tightness of this shield against external radon. This measurement is not taken into account for the estimation of the detector surface background.) For ^{212}BiPo combining the three distinct sets of dedicated background measurements, corresponding to 200.4 days of data collection and a scintillator surface area of 3.10 m^2, 29 ^{212}BiPo background events have been observed. The fitted ^{208}Tl activity for the contamination on the surface of the scintillators is $\mathcal{A}(^{208}\mathrm{Tl}) = 0.9 \pm 0.2$ μBq/m^2 of surface area of scintillator. For ^{214}BiPo combining the two distinct sets of background measurements of the two modules with the final shield, corresponding to 111.9 days of data collection and a scintillator surface area of 3.24 m^2, the fitted ^{214}Bi activity for the contamination on the surface of the scintillators is $\mathcal{A}(^{214}\mathrm{Bi}) = 1.0 \pm 0.3$ μBq/m^2 of surface area of scintillator. The background level has been controlled during sample measurements, by keeping half of the module empty and it is stable.

5. Measurement of the first SuperNEMO ^{82}Se double β source foils

The SuperNEMO foils are in the form of strips, 270 cm long, 13 cm wide and ~200 μm thick. To produce enriched ^{82}Se foils for the SuperNEMO experiment, thin and chemically purified ^{82}Se powder is mixed with Polyvinyl alcohol (PVA) glue and then deposited between Mylar foils. The Mylar foil is 12 μm thick and has been irradiated at JINR Dubna (Russia) with an ion beam and then etched in a sodium hydroxide solution. This produces a large number of microscopic holes in order to ensure a good bond and to allow water evaporation during the drying of PVA.

5.1. Analysis method

The criteria to select the *back-to-back* BiPo events and the analysis method for the ^{212}Bi and ^{214}Bi contamination measurements inside the samples is similar to the method used for the background (described in section 4.3 and 4.4). For the samples, we search for an excess of BiPo events above the background expectation in the delayed energy spectrum. The background components are random coincidences and the contamination on the scintillator surface. For the ^{82}Se foils, the contamination inside the irradiated Mylar is added as an extra component of the background. The delayed α energy spectra of the background components are then simultaneously fitted to the observed data. The surface background and the irradiated Mylar fit values are allowed to vary within the range given by the dedicated measurements. For the surface background these values are quoted in Table 2, i.e $\mathcal{A}(^{208}\mathrm{Tl}) = 0.9 \pm 0.2$ μBq/m^2, $\mathcal{A}(^{214}\mathrm{Bi}) = 1.0 \pm 0.3$ μBq/m^2 and for the irradiated Mylar they are given in section 5.2. The number of random coincidences is allowed to vary within the 1 σ range given by the expected value calculated from the single rates (as explained in section 4.4).

For the ^{214}Bi measurement, the delay time between the prompt and the delayed signal is required to be lower than 492 μs (three times the ^{214}Po half-life), to reduce the random coincidences background.

5.2. Measurement of the raw materials

Before producing the ^{82}Se foils, the raw materials have been first measured separately with the BiPo-3 detector (PVA and Mylar). The PVA is very pure in ^{208}Tl and upper limits of $\mathcal{A}(^{208}\mathrm{Tl}) < 12$ μBq/kg and $\mathcal{A}(^{214}\mathrm{Bi}) < 505$ μBq/kg are obtained (using the statistical analysis approach described in [Feldman G. J, Cousins R.D, 1998]. For the irradiated Mylar the following values are measured:

$$\begin{aligned} \mathcal{A}(^{208}\mathrm{Tl}) &= 100 \pm 53\ \mu\mathrm{Bq/kg} \\ \mathcal{A}(^{214}\mathrm{Bi}) &< 688\ \mu\mathrm{Bq/kg} \end{aligned}$$

5.3. Measurement of the enriched ^{82}Se foils

Four first SuperNEMO ^{82}Se strips with thickness ~ 40 mg/cm^2, have been measured from August 2014 to June 2015. The total duration of this measurement is 262 days for the ^{212}BiPo measurement (after rejecting the three first days to suppress the background induced by the ^{220}Rn deposition) and 241.1 days for the ^{214}BiPo measurement (after rejecting the fifteen first days to suppress the background induced by the ^{222}Rn deposition). The total effective mass of the ^{82}Se+PVA mixture is 359 g (352 g), and the effective scintillators surface area is 2.13 m^2 (1.97 m^2) for the ^{212}BiPo (^{214}BiPo) measurement. A second set of four strips with thickness ~55 mg/cm^2, have been measured from October 2015 to May 2016. The total duration of this measurement is 161.3. days for the ^{212}BiPo measurement and 109.7 days for the ^{214}BiPo measurement, the total effective mass of the ^{82}Se+PVA mixture is 777 g (726 g), and the effective scintillators surface area is 2.7 m^2 (2.52 m^2) for the ^{212}BiPo (^{214}BiPo) measurement. Combining the two set of measurement, the total duration is 423.3 days for the ^{212}BiPo measurement and 350.8 days for the ^{214}BiPo measurement.

The energy spectra of the prompt and delayed signals are presented in Figure 6. The number of fitted events

	^{212}BiPo				^{214}BiPo			
	Module 1 Temp. shield	Module 1 Final shield	Module 2 Final shield	**Combined**	Module 1 Temp. shield	Module 1 Final shield	Module 2 Final shield	**Combined Final shield**
Duration (days)	73.5	51.2	75.7	200.4	73.5	36.2	75.7	111.9
Scint. surface (m^2)	2.7	3.06	3.42	3.10	2.7	3.06	3.42	3.24
Data events	9	8	12	29	27	18	30	48
Surf. Bkg (fit)	7.4	8.0	12.0	27.7	11.7	2.5	6.9	9.4
Coinc. (fit)	1.6	0.0	0.0	1.3	15.3	15.5	23.1	38.5
Coinc. (single rate)	0.20	0.10	0.14	0.44	18.2	14.3	25.0	39.3
$\mathcal{A}$(^{208}Tl) μBq/m^2	0.8 ± 0.3	1.0 ± 0.4	1.0 ± 0.3	0.9 ± 0.2				
$\mathcal{A}$(^{214}Bi) μBq/m^2					2.5 ± 0.7	1.0 ± 0.6	1.0 ± 0.4	1.0 ± 0.3

Table 2: Results of the ^{212}BiPo and ^{214}BiPo background measurements: separate and combined results of the three dedicated background measurements.

from each background component and from bismuth contamination inside the ^{82}Se+PVA mixture are summarized in Table 3. To reject the surface background and to reduce the background contribution from the irradiated mylar, an upper limit on the delayed energy is added (700 keV for ^{212}BiPo and 600 keV for ^{214}BiPo), allowing to increase the signal over background ratio.

With a delayed energy lower than 700 keV, 18 ^{212}BiPo events are observed and 4.3 background events are expected from the fit. The excess of observed events above the fitted background is in agreement with a ^{212}Bi contamination inside the ^{82}Se+PVA mixture. Taking into account the detection efficiency of 2.65% for the first four strips and 1.55% for the second set of four strips (calculated by simulating ^{212}BiPo events emitted uniformely inside the ^{82}Se+PVA mixture), this corresponds to a 90% C.L. interval for the ^{208}Tl activity of the ^{82}Se+PVA mixture of:

$$\mathcal{A}(^{208}\mathrm{Tl}) = 20[10.5 - 32.0]\ \mu\mathrm{Bq/kg}\ (90\%\ \mathrm{C.L.})$$

For the ^{214}BiPo measurement, with a delayed energy lower than 600 keV, 87 ^{214}BiPo events are observed and 66.5 background events are expected from the fit. Taking into account the detection efficiency of 0.66% for the first four strips and 0.32% for the second set of four strips, an upper limit at 90% C.L. is set to the ^{214}Bi contamination of the ^{82}Se+PVA mixture:

$$\mathcal{A}(^{214}\mathrm{Bi}) < 290\ \mu\mathrm{Bq/kg}\ (90\%\ \mathrm{C.L.})$$

6. Conclusion

The BiPo-3 detector is a low radioactive detector dedicated to the measurement of ultra-low ^{208}Tl and ^{214}Bi contaminations in thin materials. Surface activities of $\mathcal{A}(^{208}\mathrm{Tl}) = 0.9 \pm 0.2\ \mu\mathrm{Bq/m^2}$ and $\mathcal{A}(^{214}\mathrm{Bi}) = 1.0 \pm 0.3\ \mu\mathrm{Bq/m^2}$ have been measured. It has been shown that this background can be strongly supressed by analysing the delay alpha energy spectrum. The measurement of the first SuperNEMO $\beta\beta0\nu$ source foils shows a low ^{208}Tl contamination inside the ^{82}Se mixture with an activity $\mathcal{A}(^{208}\mathrm{Tl}) = [10.5 - 32]\ \mu\mathrm{Bq/kg}$ (90% C.L.). For ^{214}Bi an upper limit (at 90% C.L.) is set $\mathcal{A}(^{214}\mathrm{Bi}) < 290\ \mu\mathrm{Bq/kg}$ (90% C.L.). The BiPo-3 detector has become a generic detector and will be available in 2017 to measure samples for various purposes.

References

Agostinelli S. et al., 2003. Geant4 - A Simulation Toolkit, Nucl. Inst. Meth. A 506, 250-303; Allison J. et al. 2006. Geant4 developments and applications, IEEE Transactions on Nuclear Science 53 No. 1, 270-278; Allison J. et al. 2016. Recent developments in Geant4, Nucl. Inst. Meth. A 835, 186-225

Arnold R. et al., 2010. Probing new physics models of neutrinoless double beta decay with SuperNEMO, Eur. Phys. J. C 70, 927-943.

Bé, M.-M. et al, 2008. Table of Radionuclides, Vol 4, ed. Bureau International des Poids et Mesures, Sèvres, France

Bé, M.-M. et al, 2004. Table of Radionuclides, Vol 2, ed. Bureau International des Poids et Mesures, Sèvres, France

Bongrand M. et al., 2011. The BiPo detector for ultralow radioactivity measurements, Proceedings Low Radioactivty Techniques, LRT Workshop, AIP Press, 1338, 49-58.

Feldman G. J. and Cousins R.D., 1998. Unified approach to the classical statistical analysis of small signals, Phys. Rev. D 57, 3873-3889.

Gomez H. et al., 2013. BiPo: A dedicated radiopurity detector for the SuperNemo experiment, Nucl. Instr. Meth. A 718, 52-55.

Ponkratenko O., Tretyak V. I., Zdesenko Y., 2000. The event generator DECAY4 for simulation of double beta processes and decay of radioactive nuclei, Phys. Atom. Nucl. 63, 1282-1287.

	^{212}BiPo				^{214}BiPo			
	$E_\alpha > 150$ keV		$150 < E_\alpha < 700$ keV		$E_\alpha > 300$ keV		$300 < E_\alpha < 600$ keV	
	Expected	Fitted	Expected	Fitted	Expected	Fitted	Expected	Fitted
Surf. Bkg.	15.6 ± 2.8	13.9	0.13 ± 0.01	0.12	5.3 ± 3.7	8.8	0.08 ± 0.05	0.12
Irrad. Mylar	21.0 ± 12.0	17.5	4.6 ± 2.5	3.8	<36	36.0	< 14.4	14.4
Rand. Coinc.	0.48	0.48	0.41	0.41	65.7 ± 8.1	71.9	47.0 ± 6.9	53.2
^{82}Se+PVA		16.8		15.1		21.2		20.5
Total Fit		48.6		19.4		137.9		88.1
Total Data		44		18		140		87

Table 3: Number of expected background events(surface background, irradiated Mylar and random coincidences) calculated from separate measurements, number of fitted events (background events and signal events from BiPo decays inside the ^{82}Se+PVA mixture) and number of observed events, after 423.3 days(350.8 days) of measurement of the first SuperNEMO ^{82}Se source foils. The number of expected and fitted events are also given in the delayed energy range $150 < E_\alpha < 700(600)$ keV allowing to reduce to zero the surface background, thus increasing the signal to noise ratio.

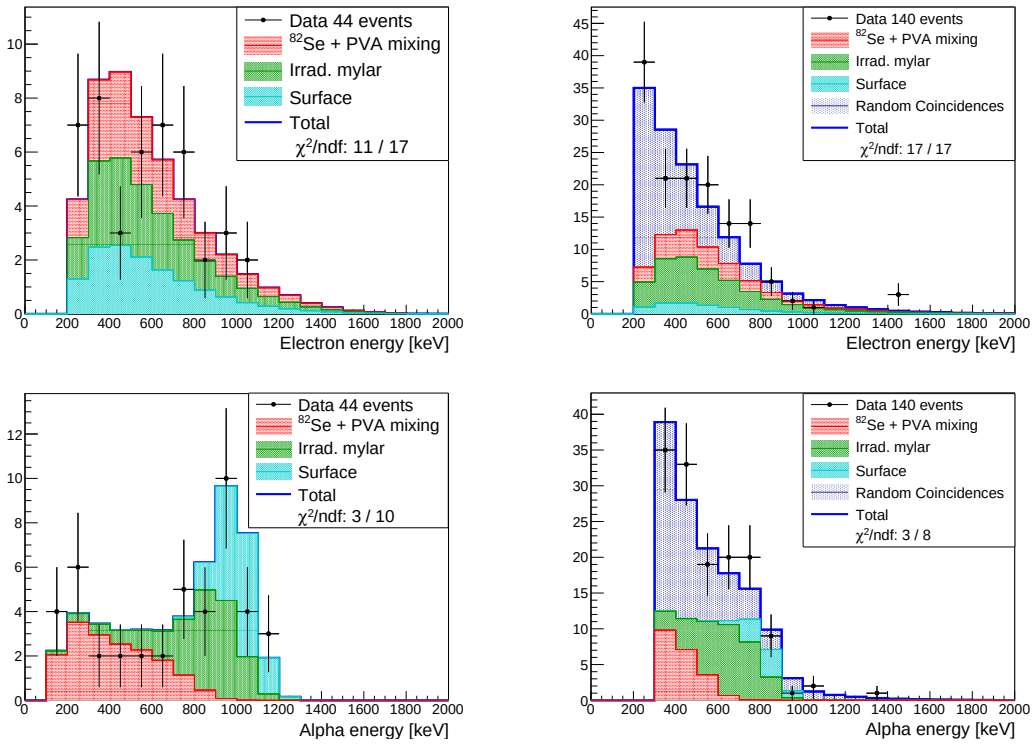

Figure 6: Distributions of the electron and alpha energy, for the ^{212}BiPo (left) and ^{214}BiPo (right) measurement of the eight first enriched ^{82}Se SuperNEMO foils, with 423.3 days and 350.8 days of data collection respectively. The data is compared to the expected background from the contamination on the surface of the scintillators (light blue histogram), the irradiated Mylar (green histogram) and random coincidences (dark blue histogram).